



OPEN

Comparative evaluation of ultrasound-assisted extraction and micelle-mediated extraction of bioactive compound from *Acmella oleracea*

Kunat Suktham¹✉, Suvimol Surassmo¹, Raweewan Thiramanas¹, Asdarina Yahya², Chaisak Chansriniyom³, Duangporn Polpanich¹ & Udom Asawapirom¹

This study compares two green extraction techniques: ultrasound-assisted extraction (UAE) and micelle-mediated extraction (MME) for isolating (2E,4E,8Z,10E)-*N*-isobutyl-2,4,8,10-dodecatetraenamide (IBDTA) from *Acmella oleracea*. EtOH was selected as the optimal solvent for UAE using Hansen solubility parameters, and extraction conditions including amplitude, extraction time, and solid-to-solvent ratio were systematically evaluated via response surface methodology. For MME, Tween 80 was used to form micelles to enhance the extraction process. The key parameters that were optimized included surfactant concentration, NaCl concentration, incubation time, and temperature. UAE achieved the highest extraction efficiency (25.94 µg/g crude extract) under 20% amplitude, 20 min, and a 1:5 solid-to-solvent ratio. MME yielded optimal extraction at 4% Tween 80, 10% NaCl, 40 min, and 80 °C, yielding 25.06 µg/g crude extract. The MME-extracted exhibited the highest anti-inflammatory activity ($IC_{50} = 52.24 \pm 5.7 \mu\text{g/mL}$), comparable to diclofenac, while maintaining moderate cytotoxicity ($IC_{50} = 1126.5 \pm 1.8 \mu\text{g/mL}$), whereas the UAE-extracted product exhibited the lowest cytotoxicity ($IC_{50} = 2513.4 \pm 1.6 \mu\text{g/mL}$) while retaining anti-inflammatory potency ($IC_{50} = 100.9 \pm 7.8 \mu\text{g/mL}$). These results highlight the suitability of both green extraction approaches for industrial-scale applications in pharmaceutical, nutraceutical and cosmeceutical industries, where there is a growing emphasis on environmentally sustainable production practices.

Keywords *Acmella oleracea*, Hansen solubility parameter, Ultrasound-assisted extraction, Micelle-mediated extraction, Response surface methodology, Green solvent

Acmella oleracea (L.) R.K. Jansen (*A. oleracea*), commonly known for its medicinal properties, belongs to the Asteraceae family and is prevalent in Brazil and other tropical and subtropical regions¹. Traditionally, it is utilized to alleviate toothache² and is widely used for wound healing, rheumatism, antimalarial and anti-inflammatory agents³. These therapeutic effects are largely attributed to bioactive components, particularly alkylamides, flavonoids, and phenolic compounds^{4,5}. Notably, spilanthol is a primary *N*-alkylamide in this plant, while another identified compound is (2E,4E,8Z,10E)-*N*-isobutyl-2,4,8,10-dodecatetraenamide (IBDTA) (Fig. 1)⁶. Despite its pharmacological importance, research focuses on optimizing the extraction conditions for IBDTA from *A. oleracea* remains limited.

When extracting targeted compounds, several factors must be considered. One of the most crucial factors is solvent selection, as it directly affects both selectivity and extractability. Previous studies have identified common solvents such as water, ethanol (EtOH), methanol (MeOH), acetone, chloroform and hexane, as well as mixtures of water with EtOH or MeOH, for extracting alkylamides from *A. oleracea*^{7–11}. However, solvents such as hexane

¹National Nanotechnology Center (NANOTEC), National Science and Technology Development Agency (NSTDA), Phahonyothin Road, Pathum Thani 12120, Thailand. ²Faculty of Chemical Engineering, Universiti Teknologi MARA (UiTM), 40450 Shah Alam, Selangor, Malaysia. ³Natural Products and Nanoparticles Research Unit, Department of Pharmacognosy and Pharmaceutical Botany, Faculty of Pharmaceutical Sciences, Chulalongkorn University, Phayathai Road, Bangkok 10330, Thailand. ✉email: kunat@nanotec.or.th

and MeOH are toxic and unsuitable for medicinal and cosmeceutical products¹². Therefore, using safer and more efficient solvents, such as EtOH or an EtOH: water mixture, is preferable for extracting IBDTA, as these solvents are less harmful to humans and the environment. Despite this, previous research has primarily focused on identifying active compounds and assessing their biological activity. To the authors' knowledge, no systematic studies have investigated the optimal extraction solvents and conditions to achieve the most efficient selective extraction of IBDTA from *A. oleracea*.

When considering the suitability of an extraction solvent for a compound of interest, solubility parameters are often crucial. Hansen solubility parameters (HSPs), which are based on three types of intermolecular forces (dispersion, polar, and hydrogen bonding), are valuable for predicting the compatibility of materials and have been widely applied across various industries^{13–16}. By utilizing this theory, it is possible to reduce time-consuming and resource-intensive screening experiments that generate large amounts of waste solvents.

In addition to solvent selection, the extraction process considerably affects compound recovery. Conventional extraction methods, such as maceration and Soxhlet extraction, are commonly employed to extract naturally derived plant compounds. However, these methods are often time-consuming, have low extraction efficiencies, and consume large quantities of solvent, which can be costly and may degrade sensitive bioactive compounds¹⁷.

Ultrasound-assisted extraction (UAE) offers a sustainable and greener alternative by using ultrasound vibrations to improve the mass transfer of bioactive constituents from plant materials into solvents¹⁸. High-intensity ultrasound waves create cavitation bubbles that physically disrupt the surface of the plant material, facilitating the release of bioactive compounds into the solvent through diffusion and dissolution¹⁹. UAE has several advantages, including high recovery rates of bioactive compounds, reduced extraction times, and low solvent usage^{20,21}. It has been successfully employed to extract a wide range of naturally derived plant substances, such as polyphenols²², polysaccharides^{21,23}, flavonoids²⁴, phenolic compounds¹⁷, lycopene²⁵, vitamins²⁶, and carotenoid²⁷ demonstrating its broad applicability.

Micelle-mediated extraction (MME) is a green extraction method used for the selective extraction or separation of organic compounds. MME utilizes micelles formed by surfactants above their critical micelle concentration to dissolve and encapsulate hydrophobic compounds within the core of the micelles (surfactant-rich phase) while leaving hydrophilic molecules in the aqueous phase²⁸. One of the advantages of MME is that the volume of the surfactant-rich phase is considerably small, resulting in a high enrichment factor, thereby improving analytical sensitivity without requiring additional steps to remove impurities or concentrate the sample²⁹.

This study is the first to optimize the extraction of IBDTA from *A. oleracea* by comparing two different green extraction methods: UAE and MME. This work advances the field by integrating solvent selection theory, extraction process optimization and comparative evaluation of green extraction strategies specifically for the target compound. In the UAE method, suitable solvents for extracting IBDTA from *A. oleracea* were systematically identified using HSPs before conducting experimental evaluations. The selected solvent was then applied in UAE. To maximize extraction efficiency, response surface methodology (RSM) was applied to optimize the extraction variables, including amplitude, extraction time, and solid-to-solvent ratio. For MME, IBDTA was extracted and separated within the micelles formed using the nonionic surfactant Tween 80 (TW80). Herein, the most suitable extraction conditions, such as surfactant concentration, extraction time, NaCl concentration, and temperature, were determined to enhance the efficiency of IBDTA extraction. To further distinguish this study from prior work, the obtained extracts were evaluated not only in terms of extraction yield but also in terms of bioactivity, focusing on cytotoxicity and anti-inflammatory effects, thereby linking the relationship between extraction efficiency with functional performance.

Materials and methods

Materials and reagents

The extraction solvents MeOH, EtOH, hexane, and acetone (99% purity) were purchased from Carlo Erba Reagents (Barcelona, Spain). All organic extraction solvents were of analytical reagent grade, while those used for chromatography were of HPLC grade. The RAW 264.7 mouse macrophage cell line was sourced from the American Type Culture Collection (ATCC, USA). Dulbecco's Modified Eagle's Medium (DMEM), L-glutamine, penicillin G sodium salt and streptomycin sulfate were purchased from GIBCO Invitrogen (NY, USA). Fetal bovine serum (FBS) was obtained from Biochrom AG (Berlin, Germany). IBDTA used as standard (IBDTA-STD) was extracted and purified at our laboratory.

Plant material

The aerial parts of *A. oleracea* were collected from Wang Saphung district, Loei province, Thailand, and one of the authors (C.C.) identified them. The herbarium specimen (CC-AO-0712) is currently stored at the Department of Pharmacognosy and Pharmaceutical Botany, Faculty of Pharmaceutical Sciences, Chulalongkorn University, Thailand. The plant materials were oven-dried at 40 °C for 3 days, then cut into small pieces and ground with a hammer mill to obtain a consistent powder. The resulting powder was stored in a sealed container at 25 °C and protected from light and humidity.

Solvent selection using HSPs theory

The HSP is made up of three energy density components: dispersion force (δ_d), polar force (δ_p), and hydrogen bonding (δ_h) parameters, which were calculated according to Eq. (1),

$$\delta_t^2 = \delta_d^2 + \delta_p^2 + \delta_h^2 \quad (1)$$

where δ_t is the total HSP parameter.

The HSP value calculations for IBDTA were performed using the Stefanis & Panayiotou group contribution method and Eqs. (2–4)³⁰:

$$\delta_d = \left(\sum_i N_i C_i + W \sum_j M_j D_j + 17.3231 \right) MPa^{1/2} \quad (2)$$

$$\delta_p = \left(\sum_i N_i C_i + W \sum_j M_j D_j + 7.3548 \right) MPa^{1/2} \quad (3)$$

$$\delta_h = \left(\sum_i N_i C_i + W \sum_j M_j D_j + 7.9793 \right) MPa^{1/2} \quad (4)$$

where C_i is the first-order group of type I , occurring N_i times within the target structure, while D_j corresponds to the second-order group of type j , which appears M_j times. The parameter W value is 0 for compounds that do not contain a second-order group and 1 for those that contain it.

To determine the solubility capacity of the solvent for the target compound, the R_a value was calculated as follows:

$$R_a = \sqrt{4(\delta_{dA} - \delta_{dB})^2 + (\delta_{pA} - \delta_{pB})^2 + (\delta_{hA} - \delta_{hB})^2} \quad (5)$$

where solvent-solute pairs with lower R_a values are expected to demonstrate higher solubility compared to those with higher R_a values.

UAE

Optimizing UAE using RSM

To optimize the extraction conditions for IBDTA from *A. oleracea*, UAE was performed using a probe-type ultrasonicator (Ultrasonic processor Q700, Qsonica, CT, USA). This device features a 0.5-inch diameter probe with a capacity of 1000 W and operates at a frequency of 20 kHz. The extraction conditions were optimized using RSM through Design Expert software (version 11.1.0.1, Stat-Ease, Minneapolis, MN, USA), using 0.5 g of dried samples. A Box–Behnken design (BBD) was employed to optimize and evaluate significant parameters during the UAE process.

Herein, three variables were examined: amplitude (ranging from 20 to 60%) as variable A, extraction time (ranging from 10 to 30 min) as variable B, and solid-to-solvent ratio (ranging from 1:5 to 1:20 (w/v)) as variable C. These variables underwent preliminary screening using a one-factor-at-a-time approach to assess their impact on extraction efficiency.

The total number of experiments in the BBD was 17, including 5 replicates at the center point to assess experimental error (Table 1). To ensure accuracy and reliability, all extraction experiments were performed in triplicate and conducted in a randomized order to minimize bias from sequence effects. The resulting extract solution was collected and then evaporated using a rotary evaporator (Rotavapor® R-100, Büchi, Switzerland). The residue extract was stored at 4 °C until analysis via HPLC.

Std	Run	Variable parameters			Responses	
		A (amplitude) %	B (extraction time) min	C (solid-to-solvent ratio) g/mL	Extraction yield %	IBDTA concentration µg/g crude extract
3	1	20	30	12.5	18.94	16.79
15	2	40	20	12.5	11.16	9.01
9	3	40	10	5	9.56	16.24
6	4	60	20	5	8.95	15.12
1	5	20	10	12.5	10.45	12.98
8	6	60	20	20	23.42	15.12
7	7	20	20	20	20.21	22.50
17	8	40	20	12.5	11.11	9.21
16	9	40	20	12.5	11.44	9.83
12	10	40	30	20	3.67	6.49
13	11	40	20	12.5	8.79	8.11
2	12	60	10	12.5	16.87	10.55
4	13	60	30	12.5	3.24	4.20
5	14	20	20	5	16.48	25.94
10	15	40	30	5	10.63	6.16
14	16	40	20	12.5	11.57	9.56
11	17	40	10	20	16.81	10.23

Table 1. Box–Behnken design (BBD) with conditions and experimentally.

The efficiency of the extraction process was assessed by examining the responses, which are influenced by different input extraction variable factors ($Y_1, Y_2, Y_3, \dots, Y_n$). The relationship between the responses and the input variables is represented by the following quadratic regression equation.

$$Y = \beta_0 + \sum_{i=1}^3 \beta_i X_i + \sum_{i=1}^3 \beta_{ii} X_i^2 + \sum_{i=1}^2 \sum_{j=i+1}^3 \beta_{ij} X_i X_j \quad (6)$$

where Y represents the predicted response, which includes extraction yield (%) and the concentration of IBDTA ($\mu\text{g/g}$ crude extract), β_0 is a constant, β_i represents the linear coefficients, β_{ii} denotes the quadratic coefficients, and β_{ij} refers to the interaction regression coefficients.

To evaluate the significance of the linear, quadratic, as well as interaction regression coefficients, analysis of variance (ANOVA) was performed, with statistical significance set at $p < 0.05$. This analysis also helped determine the validity of the quadratic models. To interpret the relationship between the dependent and independent variables, three-dimensional surface plots were created using the derived polynomial models.

MME

For the MME process, 1.0 g of dried samples was mixed with 15 mL of a specified concentration of TW80 solution (0.5–20% w/v). This mixture was subjected to ultrasonic extraction in an ultrasonic bath (Elmasonic, S60 H, Germany) at 25 °C for 20 min. The supernatant was then collected and filtered using Whatman No. 1 filter paper. A specified amount of NaCl (1–20% w/v) was then added to the solution and vortexed until completely dissolved. The cloudy solution was then incubated over a range of temperatures (40–90 °C) for a specified time (10–50 min) to allow phase separation into the aqueous phase and the surfactant-rich phase, which contained IBDTA. The surfactant-rich phase was then collected using a syringe fitted with a long needle and diluted in MeOH to reduce its viscosity. The extract was subsequently concentrated with a Rotavapor R-100 (Büchi, Switzerland), and the remaining residue was stored at 4 °C until it was analyzed by HPLC.

Scanning electron microscopy analysis (SEM)

To investigate the extent of structural degradation resulting from extraction, the powder residue of dried *A. oleracea* after extraction with UAE or MME under optimal conditions was vacuum-dried at 40 °C to remove residual solvent. The dried samples were then spread onto the surface of carbon tape and sputter-coated with gold under vacuum. The morphological features of the samples were analyzed with an environmental scanning electron microscope (ESEM, S-3400, Horiba, Japan), at an accelerating voltage of 20 kV. Observation was performed at 100–20,000 \times magnification and images were captured at 100 \times magnification to evaluate structural differences before and after extraction.

Quantitative analysis of IBDTA

Quantification of IBDTA was conducted using reverse-phase HPLC (Agilent 1260 infinity, Agilent Technologies, CA, USA). The system comprised a quaternary pump and was equipped with a 2998 photodiode array detector. Sample extracts, dissolved in MeOH at a concentration of 10 mg/mL, were pass through a 0.45- μm membrane filter before injection into a ZORBAX Eclipse XDB-C18 column (4.6 mm \times 250 mm, 5 μm , Agilent Technologies). The mobile phase comprised a gradient run of MeOH (solvent A), and water (solvent B) as follows: 50% A (0–5 min), 80% A (6–20 min), 100% A (21–25 min), and 50% A (26–30 min). The flow rate was maintained at 1.0 mL/min, with an injection volume of 10 μL and detection at 260 nm. Chromatographic peaks were determined by comparing their retention times and UV spectra with those of standard references. The chemical structure of the obtained IBDTA-STD was confirmed by ^1H -NMR (Fig. S1 and Table S1), ^{13}C -NMR (Fig. S2 and Table S2).

Cytotoxicity assay

RAW 264.7 cell line was resuspended in DMEM medium containing 10% FBS, 1% L-glutamine, and 1% penicillin/streptomycin. The cells were seeded in a 96-well plate (10,000 cells/well) and incubated at 37 °C for 24 h. After incubation, the cells were treated with various concentrations of samples for an additional 24 h. Cell viability was evaluated using the PrestoBlue™ cell viability reagent (Invitrogen, USA) following manufacturer guidelines. The untreated samples served as negative control, representing 100% cell viability, while the samples treated with 5% dimethyl sulfoxide (DMSO) served as the positive control. The half-maximal inhibitory concentration (IC_{50}), which indicates the sample concentration that inhibits cell growth by 50%, was determined by fitting a curve using nonlinear regression with the Quest Graph™ IC50 Calculator.

Anti-inflammatory activity

RAW 264.7 cells (100,000 cells/well) were plated and cultured in a 96-well plate and incubated at 37 °C for 24 h. For anti-inflammatory assay, concentration that maintained >80% cell viability as determined in the cytotoxicity assay were selected to ensure that the observed activity was not influenced by cytotoxic effects. The selected concentrations were added and incubated for an additional 2 h. Following this, the cells were treated with lipopolysaccharide (LPS) at a concentration of 1 $\mu\text{g/mL}$ for 16 h. Cell supernatants were collected and transferred to a new 96-well plate, where nitric oxide (NO) production was quantified by measuring nitrite concentrations using a modified Griess reagent according to the manufacturer's instructions. The amount of nitrite was determined using a sodium nitrite calibration curve. The percentage inhibition of NO production was calculated according to Eq. (7). Diclofenac was used as a positive control.

$$\text{Inhibition (\%)} = (A - B) \times 100 / (A - C) \quad (7)$$

Solvent	HSPs parameters (MPa $^{1/2}$) at 25 °C			R_a
	δ_d	δ_p	δ_h	
IBDTA	17.01	6.44	11.67	
Water	15.5	16.0	42.3	32.5
MeOH	14.7	12.3	22.3	13.3
EtOH	15.8	8.8	19.4	8.7
Diethyl ether	14.5	2.9	4.6	9.2
Acetone	15.5	10.4	7.0	6.7
Chloroform	17.8	3.1	5.7	6.7

Table 2. Solvent screening for the extraction of IBDTA using Hansen solubility parameter (HSP).

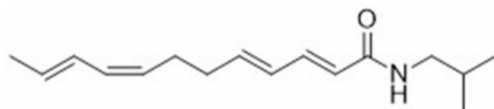


Fig. 1. Chemical structure of IBDTA.

where A, B, and C are nitrite concentrations (μM) when A: LPS (+), sample (−); B: LPS (+), sample (+); C: LPS (−), sample (−).

Statistical analysis

All experiments were performed in triplicate, with results expressed as means \pm standard deviation. Data analysis was performed using one-way ANOVA and post-hoc Tukey's test ($p < 0.05$) with IBM SPSS statistical software.

Results and discussion

Screening of suitable solvents for IBDTA

To identify the most effective solvents for extracting IBDTA from *A. oleracea*, the HSP values for commonly used pure solvents and IBDTA were calculated using the group contribution method proposed by Stefanis and Panayiotou³⁰ (Table S3) and are shown in Table 2. The results indicated that the dispersion component δ_d is the primary factor for solubilizing IBDTA, attributed to its long hydrocarbon chain and isobutyl group (Fig. 1). Additionally, the presence of amide functional groups provides opportunities for polar interactions. As shown in Table 2, the calculated R_a values from Eq. (5) suggest that IBDTA is best solubilized in solvents such as acetone and chloroform, which have low R_a values of 6.66 and 6.74 MPa $^{1/2}$, respectively. It shows moderate solubility in EtOH and diethyl ether, with R_a values of 8.74 and 9.15 MPa $^{1/2}$, respectively. By contrast, MeOH and water, which have significantly higher R_a values owing to their considerable differences in δ_h and δ_d values, are poor solvents for this compound.

Solvent evaluation

To identify the most effective green solvent for extracting IBDTA, extraction experiments were conducted using dried powdered samples of *A. oleracea* with various solvents, following the HSP prediction. Extraction was performed at 25 °C with a solid-to-solvent ratio of 1:15 (w/v) over 48 h. The highest yield was obtained with EtOH (0.3%), followed by acetone and MeOH, while water produced the lowest yield (0.2%; Fig. 2A). The extractability of the target compound IBDTA was evaluated (Fig. 2B), with EtOH providing the highest extractability, achieving a concentration of 22.75 $\mu\text{g/g}$ crude extract.

Although HSP predictions initially suggested that acetone would be the most suitable solvent owing to its lower R_a value of 6.66 MPa $^{1/2}$ compared with EtOH (8.74 MPa $^{1/2}$), MeOH (13.27 MPa $^{1/2}$), and water (32.53 MPa $^{1/2}$), the experimental results revealed that acetone extracted a slightly lower concentration of IBDTA compound (21.56 $\mu\text{g/g}$ crude extract) than EtOH. This discrepancy between theoretical solubility predictions and experimental extractability of the compound can be attributed to specific intermolecular interactions. While acetone and EtOH have comparable dispersion forces (δ_d), EtOH exhibits hydrogen bonding (δ_h) and polar interactions (δ_p) that are more closely aligned with those of IBDTA, enhancing its ability to dissolve and extract the compound more effectively. Additionally, the amphiphilic nature of EtOH enables it to interact efficiently with both the hydrophobic and hydrophilic components of the plant matrix, facilitating the better solubilization of bioactive compounds^{31,32}.

Overall, the experimental extraction results reasonably align with the solubility order predicted by the HSP theory. Consequently, EtOH yielded the highest extracts and achieved the greatest extractability of IBDTA and was selected as the most suitable solvent for further investigation.

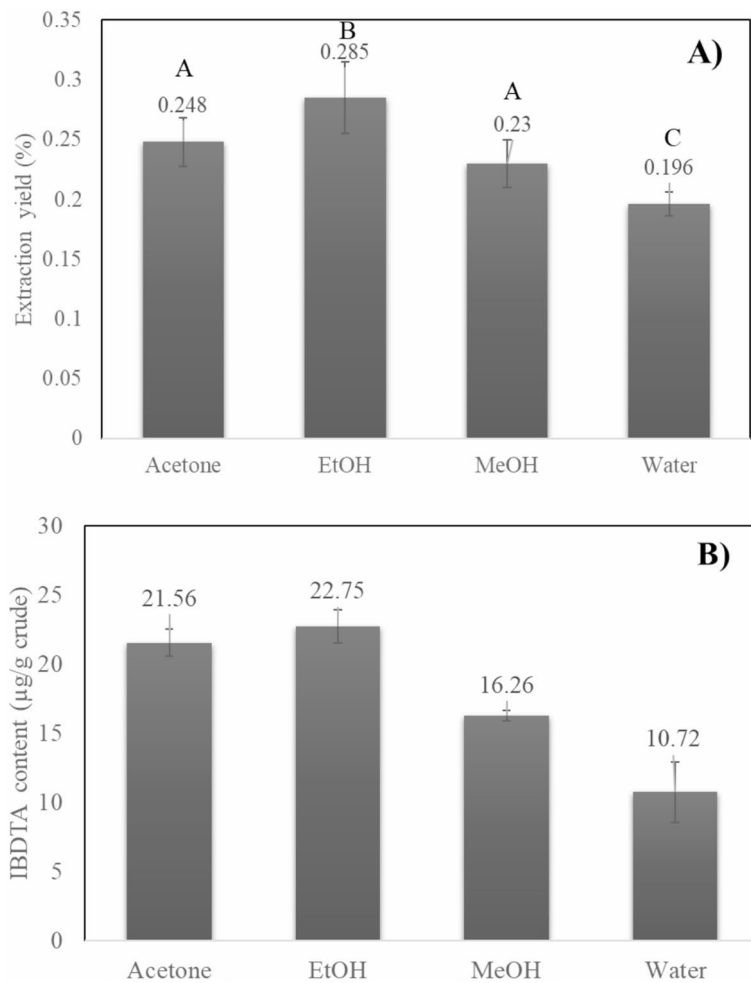


Fig. 2. Extraction yield (A) and IBDTA content (B) with candidate solvents at 25 °C for 48 h. Data represent means \pm SD ($n=3$). Different letters and symbols indicate significant differences between samples within the same category ($p < 0.05$).

Optimization of UAE via BBD-RSM

To optimize the extraction efficiency of yield and the content of IBDTA, an RSM methodology was employed using a BBD. RSM was employed to determine the influence and interactions of extraction variables. This method effectively reduced the experimental runs while enhancing the accuracy of the optimization conditions and is widely used in extraction studies^{23,33,34}. This design allowed for the systematic evaluation of three independent variables: amplitude (A), extraction time (B), and solid-to-solvent ratio (C). 17 experimental runs were performed with randomized combinations of these factors, with each variable set within its defined limits. The model's effectiveness was determined based on statistical significance ($p < 0.05$). The data were processed to create a quadratic polynomial model, leading to the derivation of mathematical regression models (Eqs. 8 and 9).

$$\begin{aligned} \text{Yield (\%)} &= 10.81 + 0.8(A) + 2.85(B) + 4.82(C) \\ &+ 0.53(AB) + 2.69(AC) + 1.46(BC) \\ &+ 4.33(A^2) + 2.23(B^2) + 2.12(C^2) \end{aligned} \quad (8)$$

$$\begin{aligned} \text{IBDTA content} &= 9.14 - 4.15(A) - 2.04(B) - 1.14(C) \\ &- 2.54(AB) + 0.86(AC) + 1.58(BC) \\ &+ 5.94(A^2) - 3.95(B^2) + 4.59(C^2) \end{aligned} \quad (9)$$

Tables 3 and 4 present the result of the ANOVA analysis, which was conducted to evaluate the statistical significance of the quadratic model at a threshold of $p < 0.05$. The coefficient of determination (R^2) values for extraction yield (0.9136) and IBDTA content (0.9637) indicate a strong correlation between predicted and observed outcomes, confirming the model's adequacy as both R^2 values exceed 0.75^{35,36}.

The significance of the models is further supported by F values of 8.22 for extraction yield and 20.65 for IBDTA content, along with p values of 0.0046 and 0.0003, respectively. These results affirm that the models are statistically significant. Additionally, the lack-of-fit analysis demonstrated that both models were insignificant

Source	Sum of squares	df	Mean square	F-value	p-value	Remark
Model	424.40	9	47.16	8.22	0.0046	Significant
A-amplitude	5.12	1	5.12	0.8924	0.3763	
B-time	64.75	1	64.75	11.29	0.0121	
C-solid ratio	185.47	1	185.47	32.33	0.0007	
AB	1.12	1	1.12	0.1958	0.6714	
AC	28.84	1	28.84	5.03	0.0599	
BC	8.47	1	8.47	1.48	0.2638	
A^2	79.05	1	79.05	13.78	0.0075	
B^2	20.90	1	20.90	3.64	0.0979	
C^2	18.99	1	18.99	3.29	0.1125	
Residual	40.16	7	5.74			
Lack of fit	34.89	3	11.63	8.83	0.0508	Not significant
R^2	0.9136					
R_{adj}^2	0.8024					

Table 3. ANOVA for the response surface quadratic model of extraction yield using UAE.

Source	Sum of squares	df	Mean square	F-value	p-value	Remark
Model	518.49	9	57.61	20.65	0.0003	Significant
A-amplitude	137.95	1	137.95	49.44	0.0002	
B-time	33.46	1	33.46	11.99	0.0105	
C-solid ratio	10.40	1	10.40	3.73	0.0949	
AB	25.81	1	25.81	9.25	0.0188	
AC	2.96	1	2.96	1.06	0.3374	
BC	10.05	1	10.05	3.60	0.0995	
A^2	148.46	1	148.46	53.21	0.0002	
B^2	67.56	1	65.76	23.57	0.0018	
C^2	88.63	1	88.63	31.77	0.0008	
Residual	19.53	7	2.79			
Lack of fit	17.80	3	5.93	13.68	0.0516	Not significant
R^2	0.9637					
R_{adj}^2	0.9170					

Table 4. ANOVA for the response surface quadratic model of IBDTA extraction using UAE.

($p > 0.05$), suggesting that the number of experiments performed was sufficient to evaluate the effects of the independent variables on the extraction yield and content of IBDTA.

Effect of UAE on extraction yield and IBDTA content

The extraction yield and content of IBDTA, as determined from 17 runs of independent variables (summarized in Table 1), revealed the influence of variable extraction. Significance was calculated using RSM. The highest extraction yield (20.21%) was achieved with an ultrasound amplitude of 20%, an extraction time of 20 min, and a solid-to-solvent ratio of 1:20 (w/v). The highest content of IBDTA was observed at an amplitude 20%, 20 min, and a ratio of 1:5 (w/v).

The three-dimensional response surface plot illustrates the interaction effects of amplitude, time, and solid-to-solvent ratio on the extraction yield and content of IBDTA in *A. oleracea* extract. The extraction yield increases with higher ultrasound amplitude and longer extraction (Fig. 3A). This enhancement is related to the disruption of plant cell walls by ultrasound, which enhances solvent penetration and facilitates the solubilization of the target bioactive compound^{37–39}. Conversely, excessively high amplitudes or prolonged extraction time may decrease the yield owing to the degradation of extraction efficiency. The interaction between amplitude and solid-to-solvent ratio, as shown in Fig. 3B, suggests that optimum yield is reached at a specific solid-to-solvent ratio, while lower or higher ratios may limit mass transfer or lead to saturation effects. Additionally, Fig. 3C shows that increasing the solid-to-solvent ratio and the extraction time enhances yield. While some of the response surface plots, particularly Fig. 3C,F, exhibit a relatively flattened curvature, this indicates that the system is approaching a plateau or saturation region where further increases in these variables do not significantly enhance the extraction yield. Overall, optimal extraction is achieved at moderate amplitude and time combined with a high solid-to-solvent ratio.

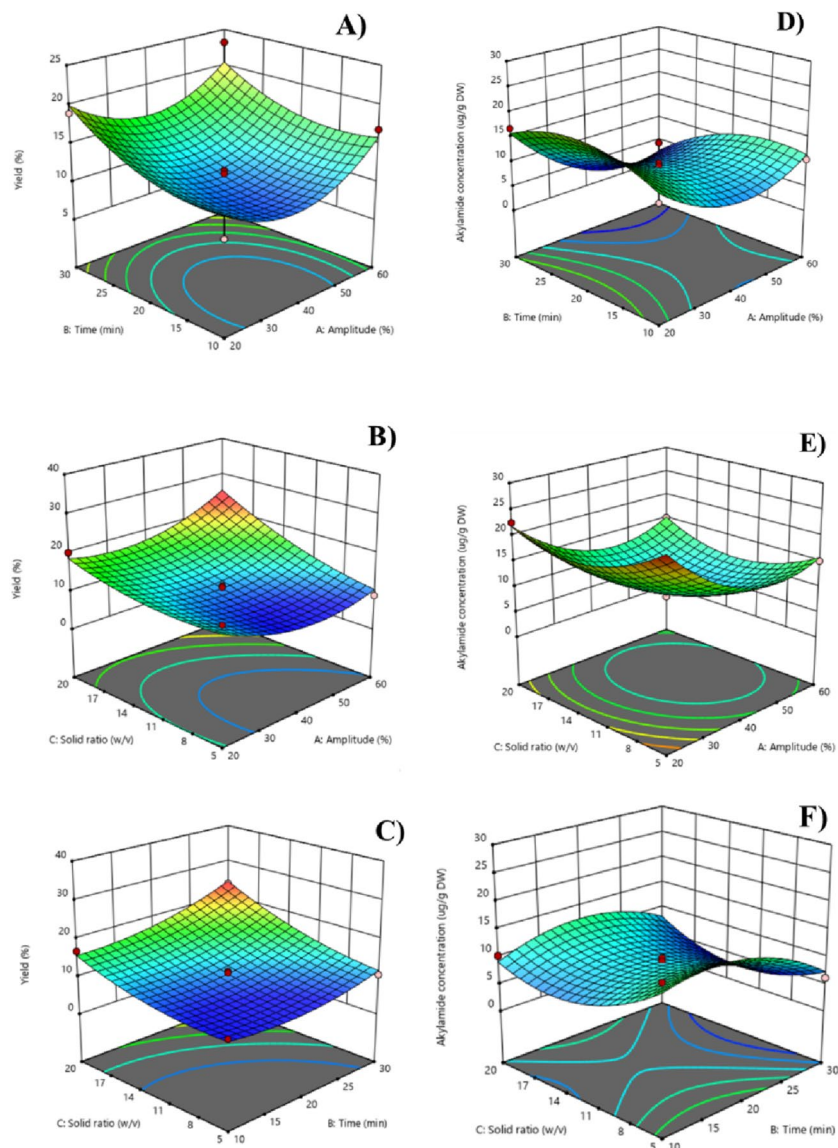


Fig. 3. Three-dimensional response surface plots illustrate the influences of variables interactions on extraction yield (A–C) and IBDTA content (D–F).

The response surface plot between amplitude and time (Fig. 3D) represents a nonlinear relationship where excessive values of amplitude and time resulted in a decrease in the content of IBDTA. This was due to thermal degradation or excessive sonication, which causes the decomposition of the compound⁴⁰. The data suggests that an optimal amplitude is necessary for enhanced extraction, as both low and high values result in decreased compound yield, potentially due to inefficient cavitation effects or solvent saturation (Fig. 3E). A low yield of IBDTA was observed at excessive solid-to-solvent ratios or long extraction times, possibly due to reduced diffusion efficiency (Fig. 3F)⁴¹. These findings emphasize the need for careful optimization of UAE conditions to maximize extraction efficiency while minimizing compound degradation.

Optimization of MME

As IBDTA exhibited low water solubility owing to its nonpolar nature, which limits its bioavailability and extraction efficiency. To enhance solubility and extraction yield, MME using surfactants presents a promising approach. In preliminary screening study, 2 non-ionic surfactants which are TW20 and TW80 were compared for their efficiency in MME of IBDTA. TW80 demonstrated significant higher extractability, achieving a recovery of 90.61% compared to TW20 (83.63%). This improved extractability is attributed to longer hydrophobic chain of TW80 (C18:1) than TW20 (C12), which forms a more hydrophobic micelle core, enhancing solubilization of the non-polar target compound. Moreover, lower HLB value (15.0 for TW80 vs. 16.7 for TW20) also represents greater affinity for hydrophobic compounds. These findings are consistent with Vinarov et al. (2018), who reported improved solubilization with increasing hydrophobic chain length across surfactant types⁴². Based

on these results, TW80 was chosen for use in the subsequent MME. Herein, extraction was performed under optimum UAE conditions, which had been previously evaluated (20% amplitude for 20 min with a solid-to-solvent ratio of 1:5 (w/v)). The effects of various parameters (TW80 concentration, NaCl concentration, incubation time, and temperature) on MME efficiency were investigated.

Effect of TW80 concentration

As shown in Fig. 4A, the yield of IBDTA in the top phase increased with increasing % TW80 from 14.29 $\mu\text{g/g}$ crude extract at 0.5% (w/v) to 24.8 $\mu\text{g/g}$ crude extract at 4% (w/v) TW80, both at 90 °C and 10% NaCl for 50 min. The critical micelle concentration (CMC) of TW80 is approximately 0.020 mM. The concentration of TW80 at 4% (w/v) (30.5 mM), are significantly above this value. The increased TW80 concentration resulted in a higher number of micelles formed, which are essential for solubilizing the target hydrophobic compound and thus may exert stronger to extract IBDTA. However, increasing the TW80 concentration to 10% (76.3 mM) did not increase extractability in the surfactant-rich (top) phase, perhaps because of limited mass transfer in high-viscosity conditions^{43,44}. Therefore, TW80 4% (w/v) was selected for further experiments.

Effect of NaCl concentration

NaCl facilitates phase separation in the MME system⁴⁵. Optimization was performed by adding NaCl at concentrations of 10–20% (w/v), as preliminary investigations had shown that no phase separation occurred at NaCl concentrations of $\leq 5\%$ (w/v). The results showed the highest yield at 10% (w/v) NaCl with 4% (w/v) TW80 at 90 °C for 50 min, yielding 25.06 $\mu\text{g/g}$ crude extract. To clarify the mechanism of this extraction behavior, micelle size distribution and zeta potential of the TW80 system were measured against NaCl concentration ranging from 0% to 20% (w/v). As shown in Fig. 5, increasing NaCl concentration increases the micelle size, from $9.41 \pm 0.06\text{ nm}$ at 0% NaCl to $121.1 \pm 1.77\text{ nm}$ at 20% NaCl. The zeta potential of the prepared micelle exhibited a shifted from $-5.42 \pm 0.31\text{ mV}$ (0% NaCl) to reach $6.06 \pm 0.71\text{ mV}$ at 20% NaCl. These data suggest the salting-out effect in which additional of NaCl increases the ionic strength of the solution resulting in compresses the electrical double layer and reduces the electrostatic repulsion between the micelles, thereby promoting their aggregation. The optimal 10% NaCl concentration demonstrates a critical balance as it provides sufficient ionic strength to induce the moderate micelle aggregation required for efficient phase separation and solubilization of the target compound. However, as the NaCl further increases to 15 and 20% (w/v), the yields decreased (Fig. 4B). This could be due to the excessive reduction in electrostatic repulsion which promotes micelle aggregation and precipitation thereby, compromising the solubility of the surfactant itself. This destabilization subsequently influenced the partition of the target compound, thereby decreasing the overall extraction efficiency. Thus, 10% (w/v) NaCl was deemed optimal for further experiments.

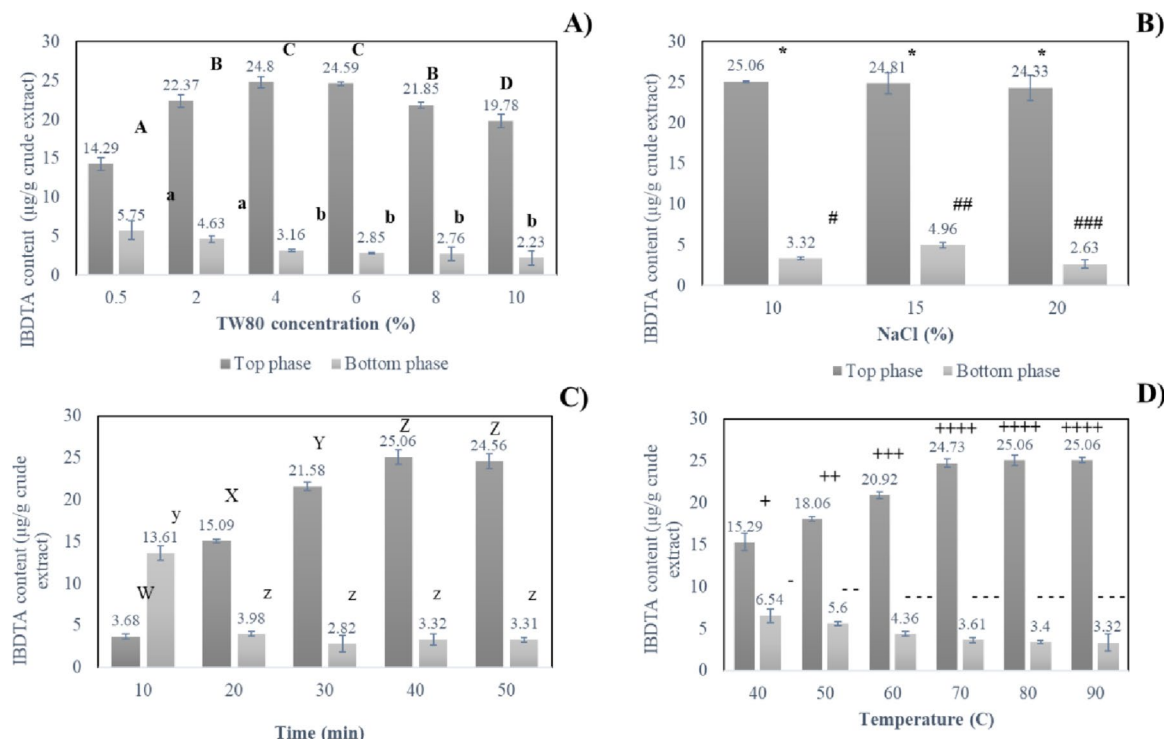


Fig. 4. Effects of (A) TW80 concentration, (B) NaCl concentration, (C) incubation time, and (D) temperature on the extraction efficiency of IBDTA using the MME approach. Conditions: (A) 10% NaCl at 90 °C for 50 min; (B) 4% TW80 at 90 °C for 50 min; (C) 4% TW80 and 10% NaCl at 90 °C and (D) 4% TW80 and 10% NaCl for 40 min. Data represent means \pm SD ($n=3$). Different symbols indicate significant differences between samples within the same category ($p < 0.05$).

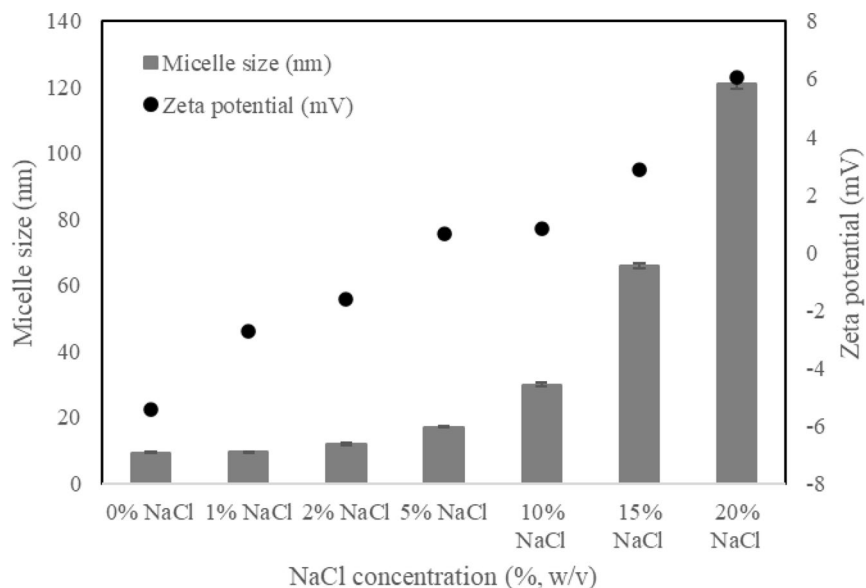


Fig. 5. Effect of NaCl concentration on micelle size and zeta potential in a system containing 4% TW 80.

Effect of incubation time

The incubation time for effective separation was assessed by varying durations from 10 to 50 min using 4% (w/v) TW80 and 10% (w/v) NaCl at 90 °C. The results indicate that the concentration of IBDTA in the surfactant-rich (top) phase increased with longer incubation times, peaking at 40 min with a concentration of 25.06 µg/g crude extract (Fig. 4C). At 50 min, there was a slight decline in concentration in the top phase. Therefore, an incubation time of 40 min was deemed optimal for this micellar extraction method.

Effect of temperature

As illustrated in Fig. 4D, the yield of IBDTA in the top phase following MME using 4% (w/v) TW80 and 10% NaCl increased significantly with temperature. At 40 °C, the concentration was 15.29 µg/g crude extract, reaching a maximum of 25.06 µg/g crude extract at 80 °C, after which the levels stabilized. Therefore, the optimal MME conditions for extracting IBDTA were determined to be 4% (w/v) TW80, 10% (w/v) NaCl, 40 min, and 80 °C.

Although the optimum extraction temperature for MME was determined to be 80 °C, there are valid concerns regarding the potential thermal degradation of the target compound. However, previous studies have shown that alkylamides, including those found in *Echinacea* species, exhibit high stability under accelerated thermal conditions up to 80 °C^{46,47}. This suggests that the alkylamide compounds are relatively resistant to heat-induced decomposition.

Destruction of the plant sample in UAE and MME

To determine the effect of UAE and MME on the structural integrity of the plant sample, SEM was used to evaluate morphological changes in plant residues. The pre-extraction sample before extraction exhibited an intact layer with visible surface integrity (Fig. 6A). Following extraction with UAE, extensive disruption of the fibrous network was observed, and the surface appeared more porous (Fig. 6B). The increased porosity indicates that UAE disrupts plant tissues through acoustic cavitation, thereby enhancing mass transfer and extraction efficiency. In the MME-extracted sample (Fig. 6C), there was more pronounced degradation of the structural matrix, with a rough and fragmented surface, indicating significant breakdown of the plant fibers. The observed morphological changes confirm that both UAE and MME significantly impact the integrity of plant material, with UAE facilitating porosity. Similarly, MME leads to extensive matrix breakdown, thereby enhancing the diffusion and recovery of bioactive constituents.

Comparison of solvent extraction, UAE, and MME

The extraction efficiency of IBDTA was evaluated using various extraction techniques and solvent systems. Maceration with different solvents, including acetone, water, MeOH, and EtOH at 25 °C, yielded concentrations of 21.56, 10.72, 16.26, and 22.75 µg/g crude extract, respectively (Table 5), with EtOH demonstrating the highest extraction efficiency. This suggests that EtOH is more effective in solubilizing and extracting the target compound owing to its compatibility with the compound's hydrophobic nature. The lower yield obtained with water can be attributed to its polarity mismatch. Further improvement was achieved through the UAE, resulting in a markedly higher yield of 25.94 µg/g crude extract under optimized conditions (20% amplitude for 20 min). This improvement is attributed to ultrasonic cavitation, which disrupts cell walls and facilitates enhanced mass transfer. Additionally, MME using TW80 micelles in an aqueous system was explored as an alternative green extraction method. MME resulted in comparable extractability to UAE, yielding 25.06 µg/g crude extract. The

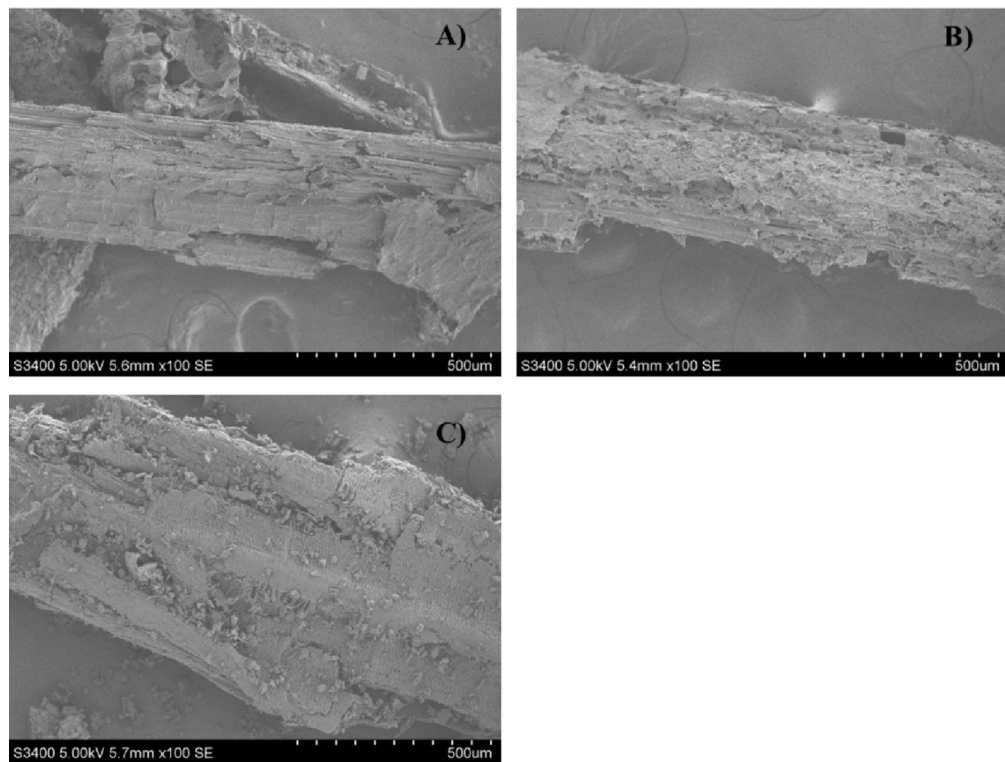


Fig. 6. ESEM images of plant residues before (A, $\times 100$) and after extraction with UAE (B, $\times 100$) and MME (C, $\times 100$).

Extraction method and solvent	Extraction condition	IBDTA ($\mu\text{g/g crude extract}$)
Maceration with		
EtOH	Batch, 25 C at solid tot solvent ratio 1:15 (w/v)	22.75 \pm 1.21*
MeOH		16.26 \pm 0.38**
Water		10.72 \pm 2.17***
Acetone		21.56 \pm 0.99*
UAE with		
EtOH	20% amplitude 20 min at a solid-to-solvent ratio of 1:20 (w/v)	25.94 \pm 2.73*
MME with		
water	4% TW80, 10% NaCl, 40 min at 80 °C	25.06 \pm 4.71*

Table 5. Comparison of solvent extraction, UAE, and MME. Data represent the mean \pm SD ($n=3$). Within the same category (column), different letters and symbols indicate significant differences between samples ($p < 0.05$).

effectiveness of MME lies in micelle formation, which improves the solubilization of hydrophobic compounds in water, facilitating efficient extraction.

Suitability of UAE and MME for industrial scale-up

Beyond the effectiveness of the extraction at the laboratory scale, the broader implications of UAE and MME for industrial application should be further evaluated. For extracting IBDTA, both UAE and MME methods significantly obtained higher yield of the compound extracts compared to conventional solvent extraction (maceration), with UAE achieving the highest yield (25.94 $\mu\text{g/g crude extract}$), followed closely by MME (25.06 $\mu\text{g/g crude extract}$). However, their differences between mechanisms and operational requirements have implications for scalability and sustainability. UAE exhibits strong potential for industrial development as its rapid processing time (20 min) and low energy inlet optimal condition (20% amplitude). UAE offers an advantage in terms of enhancing mass transfer via cavitation effect that generates microbubbles to disrupt plant cell walls and improve solvent penetration, reducing solvent usage, and maintain compound integrity. This technique has capability to implement in a continuous or semi-continuous flow setup in considerable feasible, making UAE suitable for large-scale extraction processes, where compound purity and biocompatibility are critical.

Sample	IC ₅₀ (µg/mL)	
	Cell viability	Anti-inflammatory
EtOH extract	202.1 ± 8.2*	97.0 ± 2.2 ^a
UAE extract	2513.4 ± 1.6**	100.9 ± 7.8 ^a
MME extract	1126.5 ± 1.8***	52.24 ± 5.7 ^b
Purified fraction of IBDTA	673.0 ± 3.3****	61.3 ± 3.8 ^b
Diclofenac	161.7 ± 1.3*****	55.0 ± 2.2 ^b

Table 6. In vitro anti-inflammatory and cytotoxic activities of *A. oleracea* extracts in RAW macrophage cells. Data represents the mean ± SD ($n=3$). Within the same category (column), different letters and symbols above them indicate significant differences between samples ($p<0.05$).

In contrast, MME offers a promising green alternative, using water as the solvent with nonionic surfactant (TW80) to efficiently extracting hydrophobic compounds IBDTA. MME aligns with sustainability goals, especially in food and cosmetic applications where residual organic solvents are undesirable. The use of TW80, surfactant in the Generally Recognized as Safe: GRAS), combined with high anti-inflammatory potency of the MME extracts, suggests a high potential for topical or functional food applications. However, MME process involves higher temperature (80 °C), longer extraction time (40 min), and surfactant recovery steps, which considerably complicate scaling and cost-efficiency.

In summary, UAE is considered better suited for industrial that prioritizing extraction efficiency with mild processing, while MME demonstrates a sustainable and extraction alternative with exert excellent bioactivity. The selection between these two approaches should be based on target applications, regulatory requirements and processing infrastructure.

In vitro cytotoxicity and anti-inflammatory activities

The in vitro cytotoxicity and anti-inflammatory effects of the various extracts were evaluated against RAW macrophages (Figs. S3 and S4). As shown in Table 6, the purified compound IBDTA exhibited moderate cytotoxicity with an IC₅₀ of 673.0 ± 3.3 µg/mL while demonstrating significant anti-inflammatory activity with an IC₅₀ of 61.3 ± 3.8 µg/mL. The EtOH extract exhibited lower cytotoxicity, with an IC₅₀ of 202.1 ± 8.2 µg/mL, while slightly reduce anti-inflammatory activity at an IC₅₀ of 97.0 ± 2.2 µg/mL. By contrast, the UAE extract resulted in considerably lower toxicity, with an IC₅₀ of 2513.4 ± 1.6 µg/mL, but its anti-inflammatory potential with an IC₅₀ of 100.9 ± 7.8 µg/mL was comparable with that of the EtOH extract. The MME extract exhibited moderate toxicity, with an IC₅₀ of 1126.5 ± 1.8 µg/mL but showed higher anti-inflammatory potency (IC₅₀ 52.24 ± 5.7 µg/mL), indicating a greater ability to reduce inflammation at lower concentrations compared with diclofenac, the positive control. To explore these differences, we analyzed the compositional profiles of both UAE and MME extracts. The total phenolic content (TPC) of UAE extract (2.74 ± 0.20 mg GAE/g extract) was higher than that of MME (1.80 ± 0.16 mg GAE/g extract), and the total flavonoid content (TFC) of UAE was 0.52 ± 0.16 mg QE/g extract, while that of MME extracts was not determined. HPLC chromatograms revealed that both extracts contained the same peak corresponding to our target compound. However, MME extract revealed additional minor peaks that were absent in UAE extract (Fig. S5). These findings suggest that although MME contained slightly lower amount of IBDTA and TPC, the additional minor constituents may contribute synergistically to the enhanced anti-inflammatory effect. At the same time, the higher cytotoxicity observed for MME underscores the importance of compositional complexity, as synergistic enhancement of activity also increases potential toxicity. Overall, the UAE extract demonstrated improved biocompatibility, having the lowest cytotoxicity among the crude extracts, whereas the MME extract exhibited the highest anti-inflammatory potency.

Conclusion

This study optimized the green extraction of IBDTA from *A. oleracea* using UAE and MME techniques. EtOH was selected based on HSP predictions, demonstrating superior extractability and sustainability. BBD-RSM optimization revealed that UAE conditions of 20% amplitude, 20 min, and a 1:5 (w/v) solid-to-solvent ratio achieved the highest extraction efficiency. MME, using TW80, proved effective as well, with optimal conditions at 4% (w/v) TW80, 10% (w/v) NaCl, 40 min incubation, at 80 °C. The extracts exhibited low cytotoxicity against RAW macrophage cells while retaining strong anti-inflammatory properties. This research highlights the importance of green extraction techniques in enhancing the recovery of bioactive compounds from plant sources. Future studies should assess the scalability of these methods for industrial use and their effects on compound stability and bioavailability.

Data availability

All data used in this research are available from the corresponding author upon request.

Received: 13 June 2025; Accepted: 16 December 2025

Published online: 13 January 2026

References

- Paulraj, J., Govindarajan, R. & Palpu, P. The genus spilanthes ethnopharmacology, phytochemistry, and pharmacological properties: a review. *Adv. Pharmacol. Sci.* <https://doi.org/10.1155/2013/510298> (2013).
- Sut, S. et al. Comparison of biostimulant treatments in *Acmella oleracea* cultivation for alkylamides production. *Plants (Basel)*. **9**, <https://doi.org/10.3390/plants9070818> (2020).
- Bellumori, M. et al. *Acmella Oleracea* (L.) R.K. Jansen: alkylamides and phenolic compounds in aerial parts and roots of in vitro seedlings. *J. Pharm. Biomed. Anal.* **220**, 114991. <https://doi.org/10.1016/j.jpba.2022.114991> (2022).
- Cheng, Y. B. et al. Alkylamides of *Acmella oleracea*. *Molecules*. **20**, 6970–6977 (2015).
- Nascimento, L. E. S. et al. Phytochemical profile of different anatomical parts of Jambu (*Acmella oleracea* (L.) R.K. Jansen): A comparison between hydroponic and conventional cultivation using PCA and cluster analysis. *Food Chem.* **332**, 127393. <https://doi.org/10.1016/j.foodchem.2020.127393> (2020).
- Phrutivorapongkul, A., Chaiwon, A., Vejabhikul, S., Netisingha, W. & Chansakaow, S. An anesthetic alkamide and fixed oil from *Acmella Oleracea*. *J. Health Res.* **22**, 97–99 (2018).
- Cruz, P. B. et al. Acaricidal activity of methanol extract of *Acmella oleracea* L. (Asteraceae) and spilanthol on *Rhipicephalus microplus* (Acar: Ixodidae) and *dermacentor nitens* (Acar: Ixodidae). *Vet. Parasitol.* **228**, 137–143. <https://doi.org/10.1016/j.vetpar.2016.08.026> (2016).
- Nomura, E. C. et al. Antinociceptive effects of ethanolic extract from the flowers of *Acmella oleracea* (L.) R.K. Jansen in mice. *J. Ethnopharmacol.* **150**, 583–589. <https://doi.org/10.1016/j.jep.2013.09.007> (2013).
- Paolla Raimundo, E. S. J. et al. The potential of *Acmella oleracea* as a nutraceutical source for the symptomatic treatment of burning mouth syndrome. *Nat. Prod. Res.* **38**, 3535–3541. <https://doi.org/10.1080/14786419.2023.2253974> (2024).
- Spinozzi, E. et al. Spilanthol-rich essential oil obtained by microwave-assisted extraction from *Acmella oleracea* (L.) R.K. Jansen and its nanoemulsion: Insecticidal, cytotoxic and anti-inflammatory activities. *Ind. Crop Prod.* **172**, 114027. <https://doi.org/10.1016/j.indcrop.2021.114027> (2021).
- Stein, R. et al. Chymase inhibition: A key factor in the anti-inflammatory activity of ethanolic extracts and spilanthol isolated from *Acmella oleracea*. *J. Ethnopharmacol.* **270**, 113610. <https://doi.org/10.1016/j.jep.2020.113610> (2021).
- Negi, T. et al. Deep eutectic solvents: Preparation, properties, and food applications. *Helijon* **10**, e28784. <https://doi.org/10.1016/j.helijon.2024.e28784> (2024).
- Jankovic, S. et al. Application of the solubility parameter concept to assist with oral delivery of poorly water-soluble drugs – a PEARRL review. *J. Pharm. Pharmacol.* **71**, 441–463. <https://doi.org/10.1111/jphp.12948> (2019).
- Makoni, P. A., Ranchhod, J., WaKasongo, K., Khamanga, S. M. & Walker, R. B. The use of quantitative analysis and Hansen solubility parameter predictions for the selection of excipients for lipid nanocarriers to be loaded with water soluble and insoluble compounds. *Saudi Pharm. J.* **28**, 308–315. <https://doi.org/10.1016/j.jsps.2020.01.010> (2020).
- Patel, K. G. et al. Experimentally determined Hansen solubility parameters of biobased and biodegradable polyesters. *ACS Sustain. Chem. Eng.* **12**, 2386–2393. <https://doi.org/10.1021/acsschemeng.3c07284> (2024).
- Fernandes, C. C., Paiva, A., Haghbaksh, R. & Duarte, A. R. C. Application of Hansen solubility parameters in the eutectic mixtures: difference between empirical and semi-empirical models. *Sci. Rep.* **15**, 3862. <https://doi.org/10.1038/s41598-025-8705-0> (2025).
- Diwathe, M. C., Mazumdar, B. & J, A. & Optimization of ultrasound-assisted extraction of phenolics from *Cordia dichotoma* leaves using response surface methodology. *Chem. Eng. Res. Des.* **208**, 572–587. <https://doi.org/10.1016/j.cherd.2024.07.016> (2024).
- Jha, A. K. & Sit, N. Extraction of bioactive compounds from plant materials using combination of various novel methods: A review. *Trends Food Sci. Technol.* **119**, 579–591. <https://doi.org/10.1016/j.tifs.2021.11.019> (2022).
- Shi, X. et al. Ultrasound wave assisted removal of ceftriaxone sodium in aqueous media with novel nano composite g-C3N4/MWCNT/Bi2WO6 based on CCD-RSM model. *Ultrason. Sonochem.* **68**, 104460. <https://doi.org/10.1016/j.ultsonch.2019.01.018> (2020).
- Chen, G. et al. High-pressure ultrasonic-assisted extraction of polysaccharides from mentha haplocalyx: Structure, functional and biological activities. *Ind. Crops Prod.* **130**, 273–284. <https://doi.org/10.1016/j.indcrop.2018.12.086> (2019).
- Rossbach, V., Padoin, N., Meier, H. F. & Soares, C. Influence of ultrasonic waves on the gas-solid flow and the solids dispersion in a CFB riser: numerical and experimental study. *Powder Technol.* **389**, 430–449. <https://doi.org/10.1016/j.powtec.2021.05.051> (2021).
- Gao, Y. et al. A green ultrasound-assisted enzymatic extraction method for efficient extraction of total polyphenols from empetrum nigrum and determination of its bioactivities. *J. Ind. Eng. Chem.* **109**, 559–567. <https://doi.org/10.1016/j.jiec.2022.02.041> (2022).
- Yang, S., Li, X. & Zhang, H. Ultrasound-assisted extraction and antioxidant activity of polysaccharides from *tenebrio molitor*. *Sci. Rep.* **14**, 28526. <https://doi.org/10.1038/s41598-024-79482-0> (2024).
- Wang, Q. et al. Optimization of ultrasound-assisted deep eutectic solvents extraction of Rutin from *ilex Asprella* using response surface methodology. *Sci. Rep.* **15**, 6205. <https://doi.org/10.1038/s41598-025-90536-9> (2025).
- Marinaccio, L. et al. Ultrasound assisted lycopene extraction from tomato skin waste by volatile natural deep eutectic solvent. *Food Chem. Adv.* **4**, 100656. <https://doi.org/10.1016/j.jocha.2024.100656> (2024).
- Patil, J., Ghodke, S., Jain, R. & Dandekar, P. Extraction of vitamin D from button mushroom (*Agaricus bisporus*) using deep eutectic solvent and ultrasonication. *ACS Sustain. Chem. Eng.* **6**, 10578–10586. <https://doi.org/10.1021/acsschemeng.8b01915> (2018).
- Sebdani, M. M. & Abbasi, H. Green extraction of carotenoids from pumpkin with ultrasound-assisted method; optimization using response surface methodology. *Microchem. J.* **193**, 109092. <https://doi.org/10.1016/j.microc.2023.109092> (2023).
- Suktham, K., Surassmo, S., Chansriniyom, C., Goto, M. & Shotiprak, A. Enhancing anti-diabetic activity and reducing cytotoxicity of *T. crispa* extracts through sustainable approach of pressurized hot water extraction and micelle-mediated separation. *J. Supercrit. Fluids*. **214**, 106377. <https://doi.org/10.1016/j.supflu.2024.106377> (2024).
- Xing, W. & Chen, L. Micelle-mediated extraction and cloud point preconcentration of Bergenin from *Ardisia japonica*. *Sep. Purif. Technol.* **110**, 57–62. <https://doi.org/10.1016/j.seppur.2013.03.004> (2013).
- Stefanis, E. & Panayiotou, C. Prediction of Hansen solubility parameters with a new group-contribution method. *Int. J. Thermophys.* **29**, 568–585. <https://doi.org/10.1007/s10765-008-0415-z> (2008).
- Ballal, D. & Chapman, W. G. Hydrophobic and hydrophilic interactions in aqueous mixtures of alcohols at a hydrophobic surface. *J. Chem. Phys.* **139** <https://doi.org/10.1063/1.4821604> (2013).
- Klemm, W. R. & Williams, H. J. Amphiphilic binding site of ethanol in reversed lipid micelles. *Alcohol* **13**, 133–138. [https://doi.org/10.1016/0741-8329\(95\)02024-1](https://doi.org/10.1016/0741-8329(95)02024-1) (1996).
- Roosta, M., Ghaedi, M., Daneshfar, A., Sahraei, R. & Asghari, A. Optimization of combined ultrasonic assisted/tin sulfide nanoparticle loaded on activated carbon removal of erythrosine by response surface methodology. *J. Ind. Eng. Chem.* **21**, 459–469. <https://doi.org/10.1016/j.jiec.2014.03.005> (2015).
- Morán-Aguilar, M. G. et al. Enhancing the biorefinery of brewery spent grain by deep eutectic solvent pretreatment: optimisation of polysaccharide enrichment through a response surface methodology. *J. Ind. Eng. Chem.* **145**, 693–704. <https://doi.org/10.1016/j.jiec.2024.10.066> (2025).
- Chauhan, B. & Gupta, R. Application of statistical experimental design for optimization of alkaline protease production from *Bacillus* sp. RGR-14. *Process. Biochem.* **39**, 2115–2122. <https://doi.org/10.1016/j.procbio.2003.11.002> (2004).
- Thakker, M., Parikh, J. & Desai, M. Ultrasound assisted hydrotropic extraction: a greener approach for the isolation of geraniol from the leaves of *Cymbopogon martinii*. *ACS Sustain. Chem. Eng.* **6** <https://doi.org/10.1021/acsschemeng.7b03374> (2018).

37. Chemat, F. et al. Ultrasound assisted extraction of food and natural products. Mechanisms, techniques, combinations, protocols and applications. A review. *Ultrason. Sonochem.* **34**, 540–560. <https://doi.org/10.1016/j.ultsonch.2016.06.035> (2017).
38. Khalid, W. et al. Influence of ultrasound-assisted extraction of bioactives from Garlic (*Allium sativum*) sprouts using response surface methodology. *Ultrason. Sonochem.* **115**, 107286. <https://doi.org/10.1016/j.ultsonch.2025.107286> (2025).
39. Saleh, I. A. et al. A possible general mechanism for ultrasound-assisted extraction (UAE) suggested from the results of UAE of chlorogenic acid from *Cynara scolymus* L. (artichoke) leaves. *Ultrason. Sonochem.* **31**, 330–336. <https://doi.org/10.1016/j.ultsonch.2016.01.002> (2016).
40. Pedisić, S. et al. Efficiency of microwave and ultrasound-assisted extraction as a green tool for polyphenolic isolation from *Monofloral honeys*. *Processes* **11**, 3141 (2023).
41. Zhang, Q. W., Lin, L. G. & Ye, W. C. Techniques for extraction and isolation of natural products: a comprehensive review. *Chin. Med.* **13**, 20. <https://doi.org/10.1186/s13020-018-0177-x> (2018).
42. Vinarov, Z., Dobreva, P. & Tcholakpva, S. Effect of surfactant molecular structure on progesterone solubilization. *J. Drug Del. Sci. Tech.* **43**, 44–49. <https://doi.org/10.1016/j.jddst.2017.09.014> (2008).
43. Guo, N. et al. Application of integrative cloud point extraction and concentration for the analysis of polyphenols and alkaloids in mulberry leaves. *J. Pharm. Biomed. Anal.* **167**, 132–139. <https://doi.org/10.1016/j.jpba.2019.02.002> (2019).
44. Szymczyk, K. & Taraba, A. Aggregation behavior of triton X-114 and tween 80 at various temperatures and concentrations studied by density and viscosity measurements. *J. Therm. Anal. Calorim.* **126**, 315–326. <https://doi.org/10.1007/s10973-016-5631-3> (2016).
45. Srinivasan, R., Chandrasekar, M. J. N., Nanjan, M. J. & Suresh, B. Antioxidant activity of *Caesalpinia digyna* root. *J. Ethnopharmacol.* **113**, 284–291. <https://doi.org/10.1016/j.jep.2007.06.006> (2007).
46. Liu, Y. & Murohy, P. A. Alkamide stability in *Echinacea purpurea* extracts with and without phenolic acids in dry films and in solution. *J. Agric. Food Chem.* **55**, 120–126. <https://doi.org/10.1021/jf0619481> (2007).
47. Stuart, D. L. & Wills, R. B. Effect of drying temperature on alkylamide and cichoric acid concentrations of *Echinacea purpurea*. *J. Agric. Food Chem.* **51**, 1608–1610. <https://doi.org/10.1021/jf026213k> (2003).

Author contributions

K.S. : Conceptualization, data curation, investigation, methodology, validation, writing-original draft and writing-review and editing. R.W., A.Y., S.S. and C.C.: Methodology and formal analysis. D.P. and U.A.: Funding acquisition and project administration.

Funding

The work was supported by National Nanotechnology Center, National Science and Technology Development Agency (NSTDA); Thailand Science Research and Innovation (TSRI), and National Science, Research and Innovation Fund (NSRF) (P2451312).

Declarations

Competing interests

The authors declare no competing interests.

The authors declare that they have no known competing interest.

Additional information

Supplementary Information The online version contains supplementary material available at <https://doi.org/10.1038/s41598-025-33115-2>.

Correspondence and requests for materials should be addressed to K.S.

Reprints and permissions information is available at www.nature.com/reprints.

Publisher's note Springer Nature remains neutral with regard to jurisdictional claims in published maps and institutional affiliations.

Open Access This article is licensed under a Creative Commons Attribution-NonCommercial-NoDerivatives 4.0 International License, which permits any non-commercial use, sharing, distribution and reproduction in any medium or format, as long as you give appropriate credit to the original author(s) and the source, provide a link to the Creative Commons licence, and indicate if you modified the licensed material. You do not have permission under this licence to share adapted material derived from this article or parts of it. The images or other third party material in this article are included in the article's Creative Commons licence, unless indicated otherwise in a credit line to the material. If material is not included in the article's Creative Commons licence and your intended use is not permitted by statutory regulation or exceeds the permitted use, you will need to obtain permission directly from the copyright holder. To view a copy of this licence, visit <http://creativecommons.org/licenses/by-nc-nd/4.0/>.

© The Author(s) 2026